CHAPTER IV

RESULT AND DISCUSSION

4.1 Shape of PMMA, PMMA-Co-PEMA, $BaSO_4$, HAP investigated by SEM

Figures 4.1 and 4.2 show particle shape and size distribution of $BaSO_4$ and hydroxyapatite (HAP) respectively. It was observed that both $BaSO_4$ and HAP had hexagonal shape and agglomerate distribution. Due to the particles distributed in the form of agglomeration, particle size shown in the scanning electron microscope (SEM) photograph was smaller than the particle size detected by particle size analyzer as shown in Figure 3.1 and 3.2

Figure 4.1 SEM photograph of $BaSO_4$ particle (a) x 1.0 k (b) x 20 k

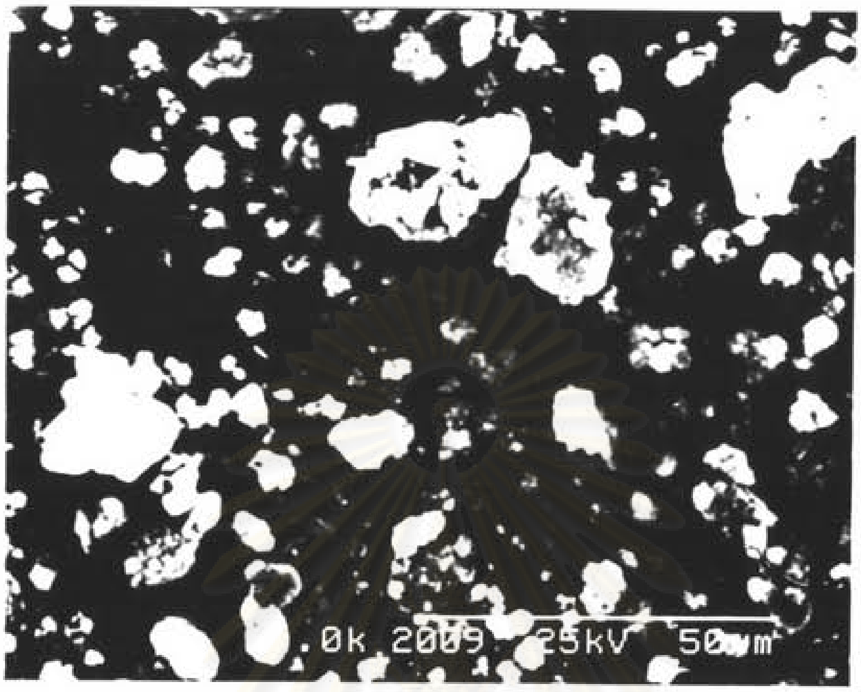

(a)

(b)

Figure 4.2 SEM photograph of untreated hydroxyapatite particles

(a) x 1.0 k (b) x 50 k

Shape and size of PMMA and PMMA-Co-PEMA were shown in Figures 4.3-4.4. Both of the polymer beads were shown to have spherical shape and homogeneous distribution. In case of hydroxyapatite reinforced PMMA or PMMA-Co-PEMA bone cement, it was observed that either silane treated or untreated hydroxyapatite still distributed in the form of agglomeration as shown in Figure 4.5 and 4.6 respectively.

Figure 4.3 SEM photograph x 100 of PMMA powder

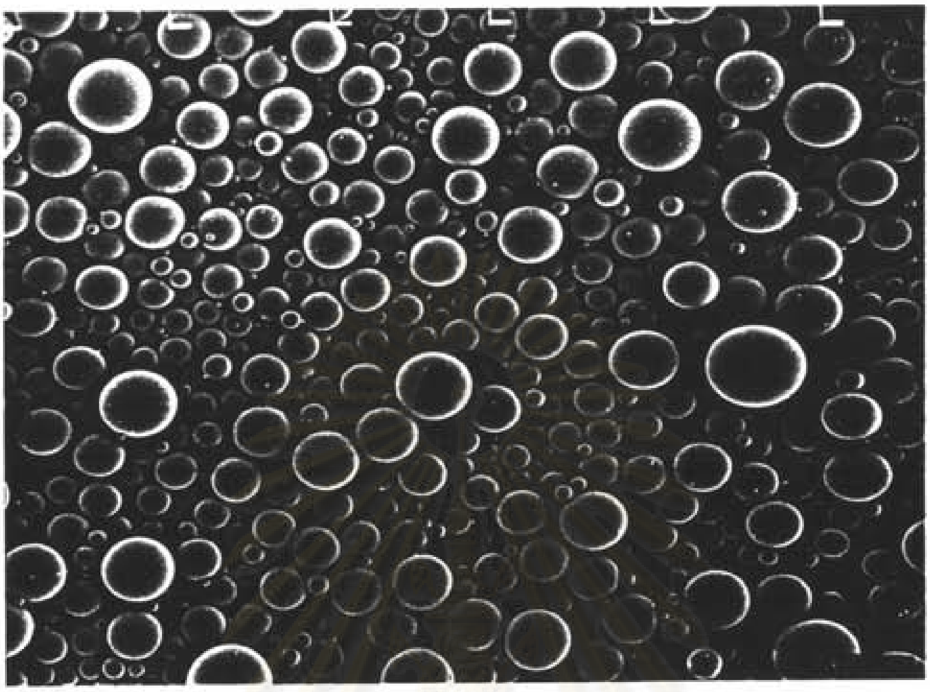

Figure 4.4 SEM photograph x 100 of PMMA-Co-PEMA powder

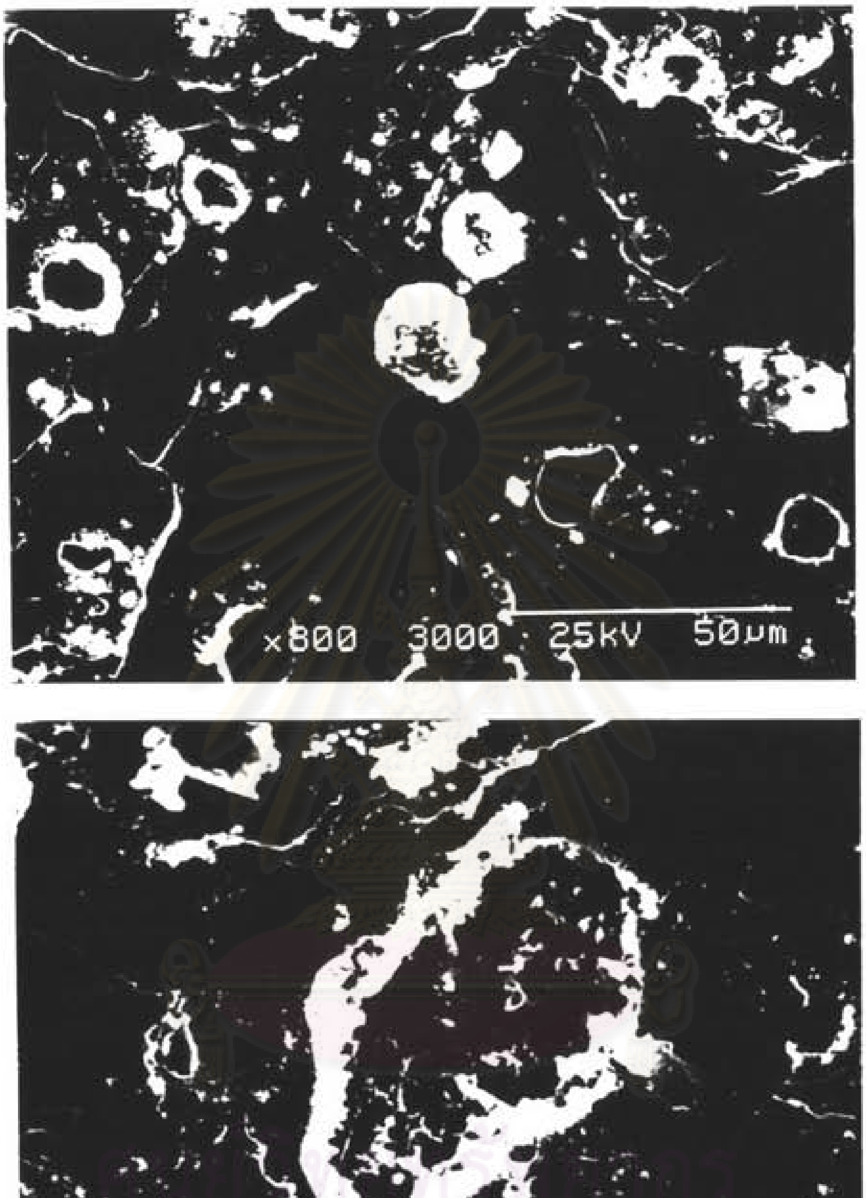

(a)

(b)

Figure 4.5 SEM photograph of fractured sample of untreated hydroxyapatite reinforced PMMA-Co-PEMA bone cement (a) x 800 (b) x 1.0 k

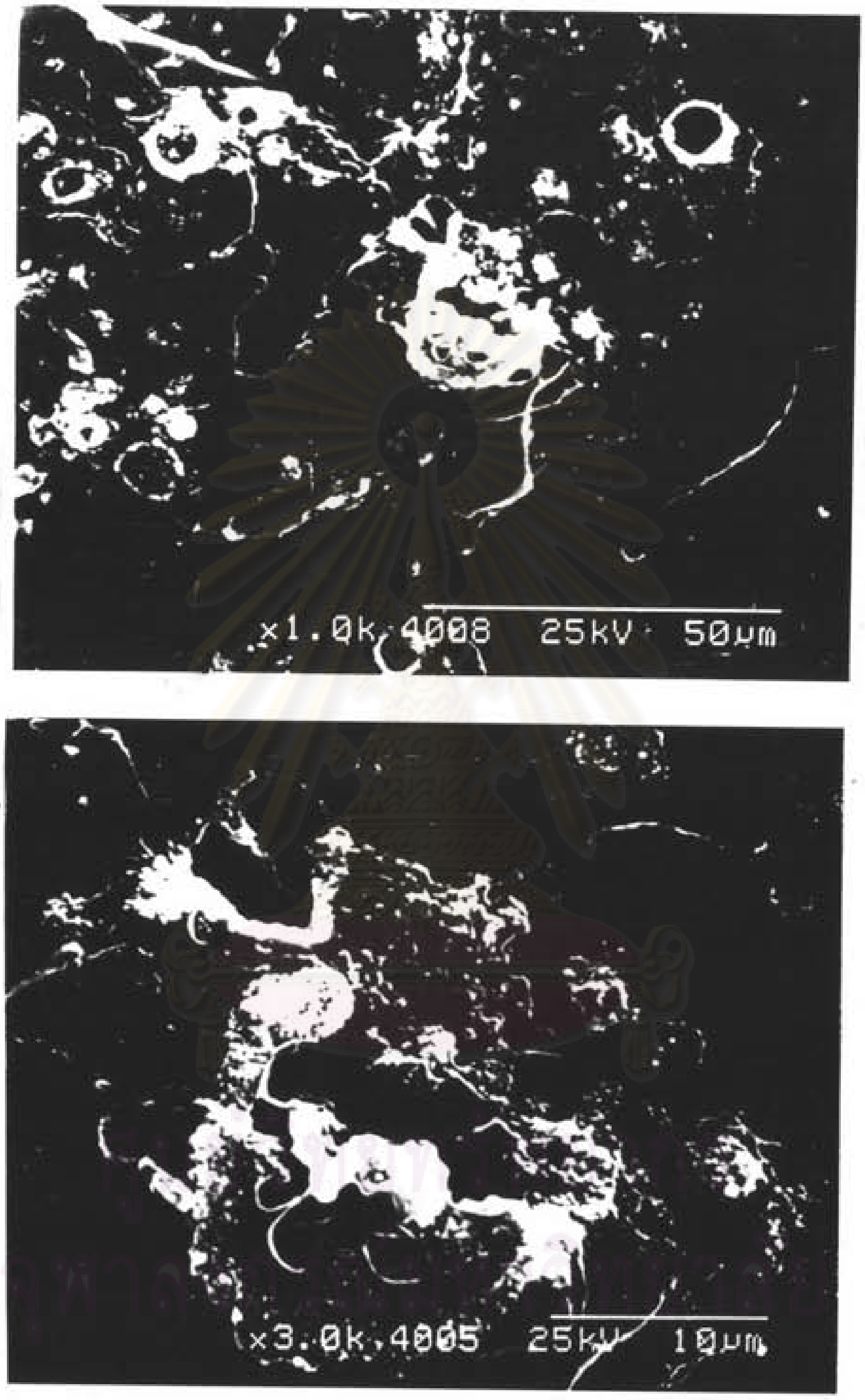

(a)

(b)

Figure 4.6 SEM photograph of fractured sample of silane treated hydroxyapatite reinforced PMMA-Co-PEMA bone cement (a) x 1.0 k (b) x 3 k

4.2 FT-IR Characterization of Silane Coupling Agent on HAP

Silane coupling agent reacts on surface hydroxyapatite as shown below.

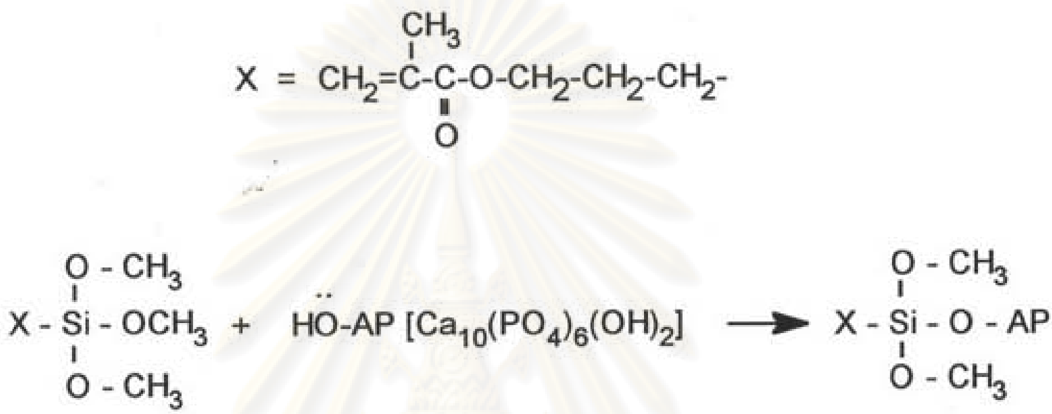

Hydroxyapatite

3-trimethoxysilylpropylmethacrylate

Figure 4.7 shows FT-IR spectra of hydroxyapatite before and after treatment with silane coupling agent and illustrates absorption bands of C=O at approximately 1720 cm^{-1}, C=C bands at 1630 cm^{-1}, and Si-O bands at 1300 to 1250 cm^{-1} indicating the availability of the silane coupling groups on the surface of hydroxyapatite.

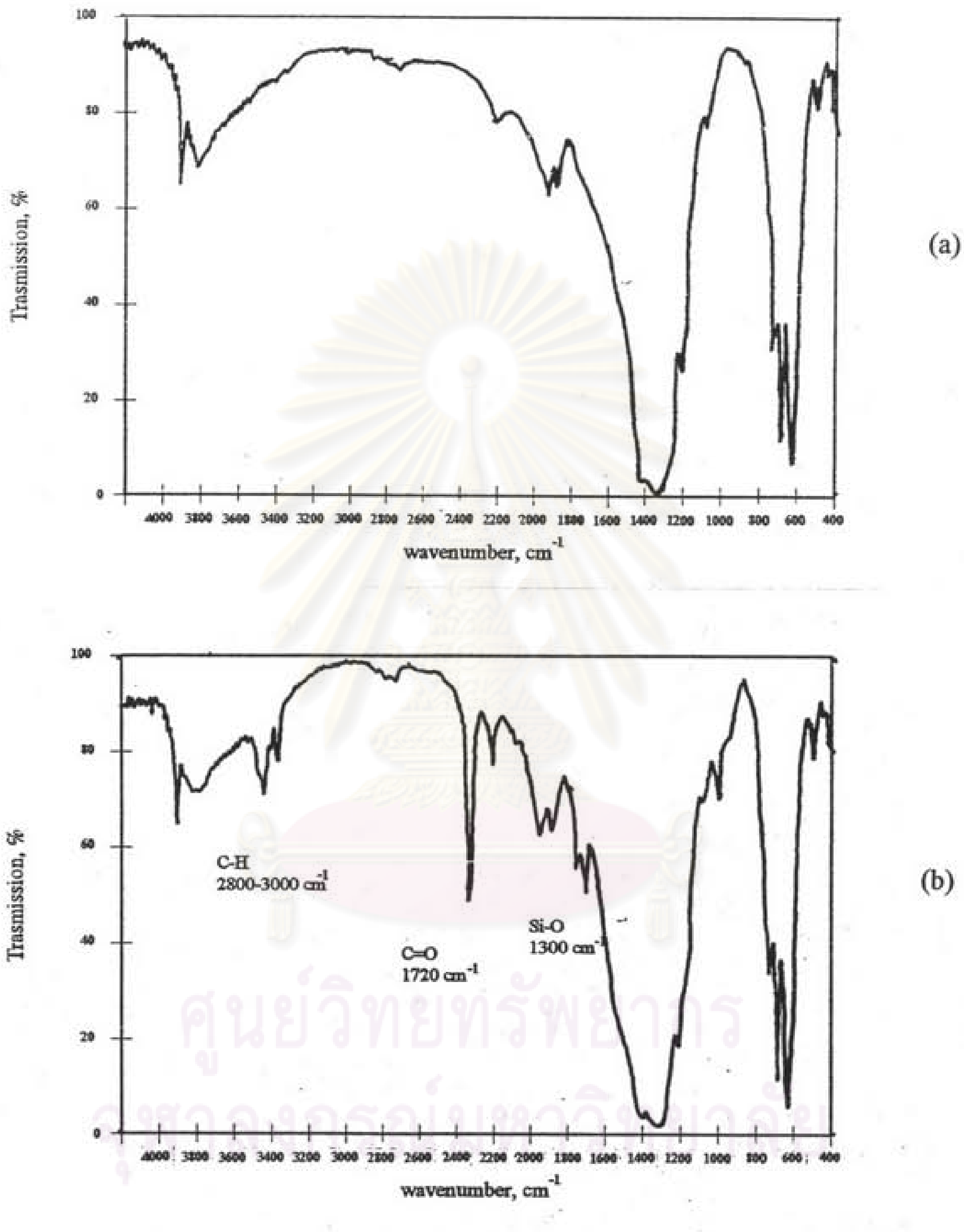

Figure 4.7 FT-IR spectra of hydroxyapatite before (a) and after (b) silane surface treatment

4.3 Determination of Silane Coupling Agent Content on HAP

The silane coupling agent content on hydroxyapatite was determined by burning at 550°C so that organic part of silane decomposes, then, calculated a real content of silane from weight loss, as shown in Table 4.1 (method of calculation is described in appendix B).

Table 4.1 Silane coupling agent content in hydroxyapatite

Sample No.	Silane solution, % by volume of solution	Silane content % by weight of HAP
1	0.5	3.72
2	1	5.21
3	2	7.83

4.4 Mechanical Properties of $BaSO_4$ Reinforced PMMA Bone cement

Dependence of mechanical properties of PMMA bone cement upon $BaSO_4$ content was shown in Table 4.2 and Figure 4.8. It was observed that though the yield stress of the bone cement decreased with the increasing weight percent of $BaSO_4$, the Young's modulus increased from 3269 to 4538 MPa for 0-40 weight percent ranges of $BaSO_4$. The results indicates the brittle nature or low modulus materials of the PMMA of which the modulus increased with amount of higher modulus reinforcement.

Table 4.2 Tensile properties of $BaSO_4$ reinforced PMMA

$BaSO_4$ %	Stress, MPa (at max. load)		Strain to failure, %		Modulus, MPa	
0	49.62	(4.89)	2.32	(16.03)	3269	(13.87)
10	45.07	(6.42)	1.93	(18.24)	3772	(16.56)
20	43.80	(11.32)	1.73	(20.53)	3997	(14.36)
30	39.04	(8.44)	1.42	(16.17)	4196	(12.29)
40	35.82	(4.38)	1.01	(12.80)	4538	(13.25)

NOTE : ( ) is coefficient of variation

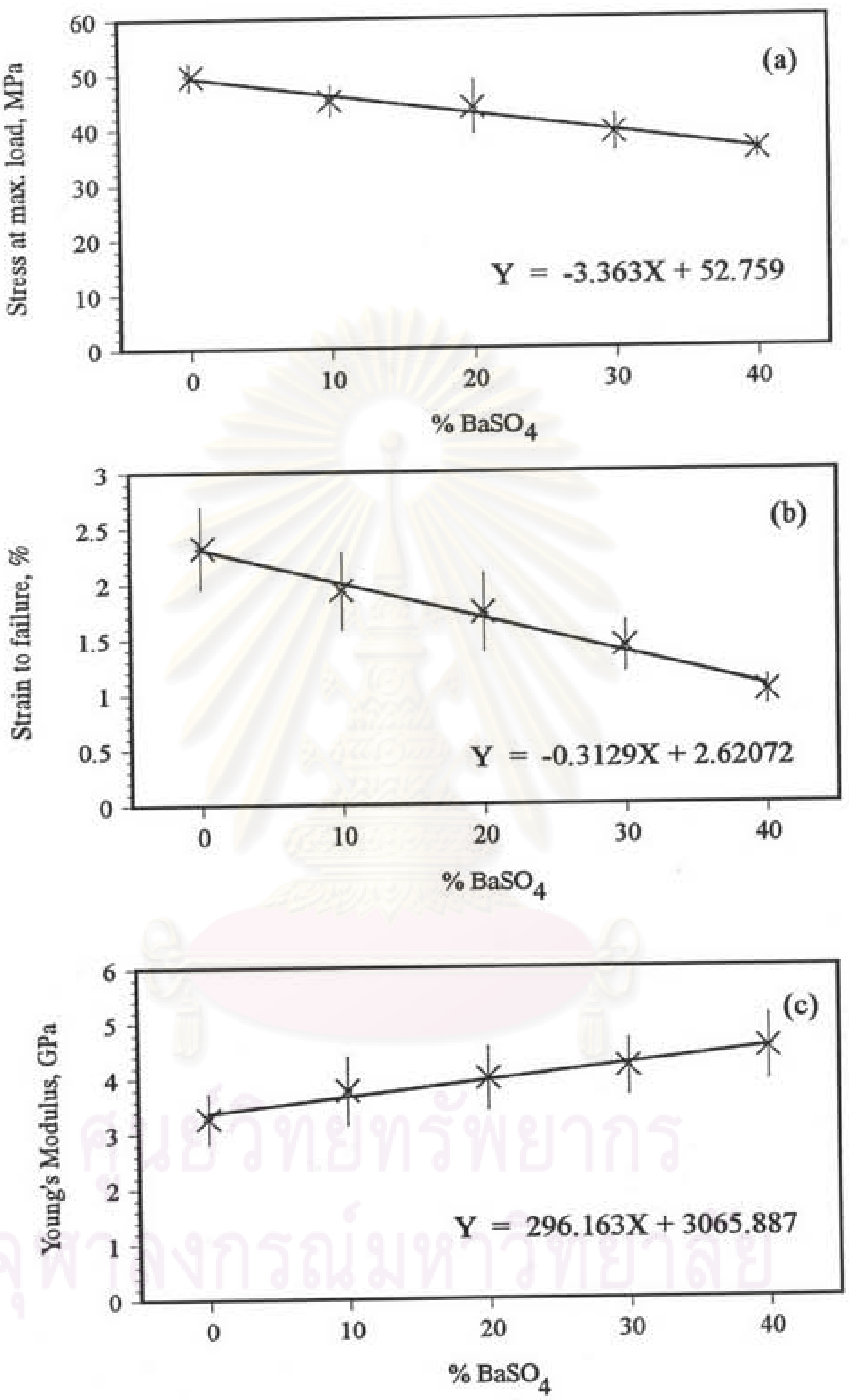

Figure 4.8 Tensile properties of PMMA dependence with increasing percent weight of $BaSO_4$ (a) Stress at maximum load (b) Strain to failure (c) Young's modulus

4.5 Mechanical Properties of $BaSO_4$ Reinforced PMMA-Co-PEMA Bone Cement

Comparison of tensile properties of PMMA-Co-PEMA bone cement to those of the conventional PMMA bone cement was shown in Table 4.3. The slightly higher Young's modulus of the PMMA-Co-PEMA bone cement, but lower yield stress, was considered as a result of PEMA moiety in the polymer chains. However, the Young's modulus of the copolymer can be improved by reinforced with some particulate reinforcements. Tensile properties of the $BaSO_4$ reinforced copolymer bone cement was shown in Table 4.4 and Figure 4.9. The Young's modulus was found to increase upto 34.9 % from 3453 MPa to 4658 MPa for 0-40 weight percent ranges of $BaSO_4$.

Table 4.3 Comparison of tensile properties of PMMA-Co-PEMA to PMMA bone cement

	Stress, MPa (at max. load)		Strain to failure, %		Modulus, MPa	
PMMA	49.62	(4.89)	2.32	(16.03)	3269	(13.87)
PMMA-Co-PEMA	48.77	(8.89)	2.26	(19.93)	3453	(12.09)

NOTE : ( ) is coefficient of variation

Table 4.4 Tensile properties of $BaSO_4$ reinforced PMMA-Co-PEMA

$BaSO_4$ %	Stress, MPa (at max. load)		Strain to failure, %		Modulus, MPa	
0	48.77	(8.89)	2.26	(19.93)	3453	(12.09)
5	46.28	(3.21)	2.06	(7.51)	3635	(4.00)
10	44.93	(9.30)	1.95	(21.77)	3862	(10.71)
20	40.45	(4.38)	1.58	(13.90)	4122	(8.23)
30	35.09	(5.46)	1.34	(19.13)	4265	(6.37)
40	32.35	(7.32)	1.01	(16.99)	4660	(10.64)

NOTE : ( ) is coefficient of variation

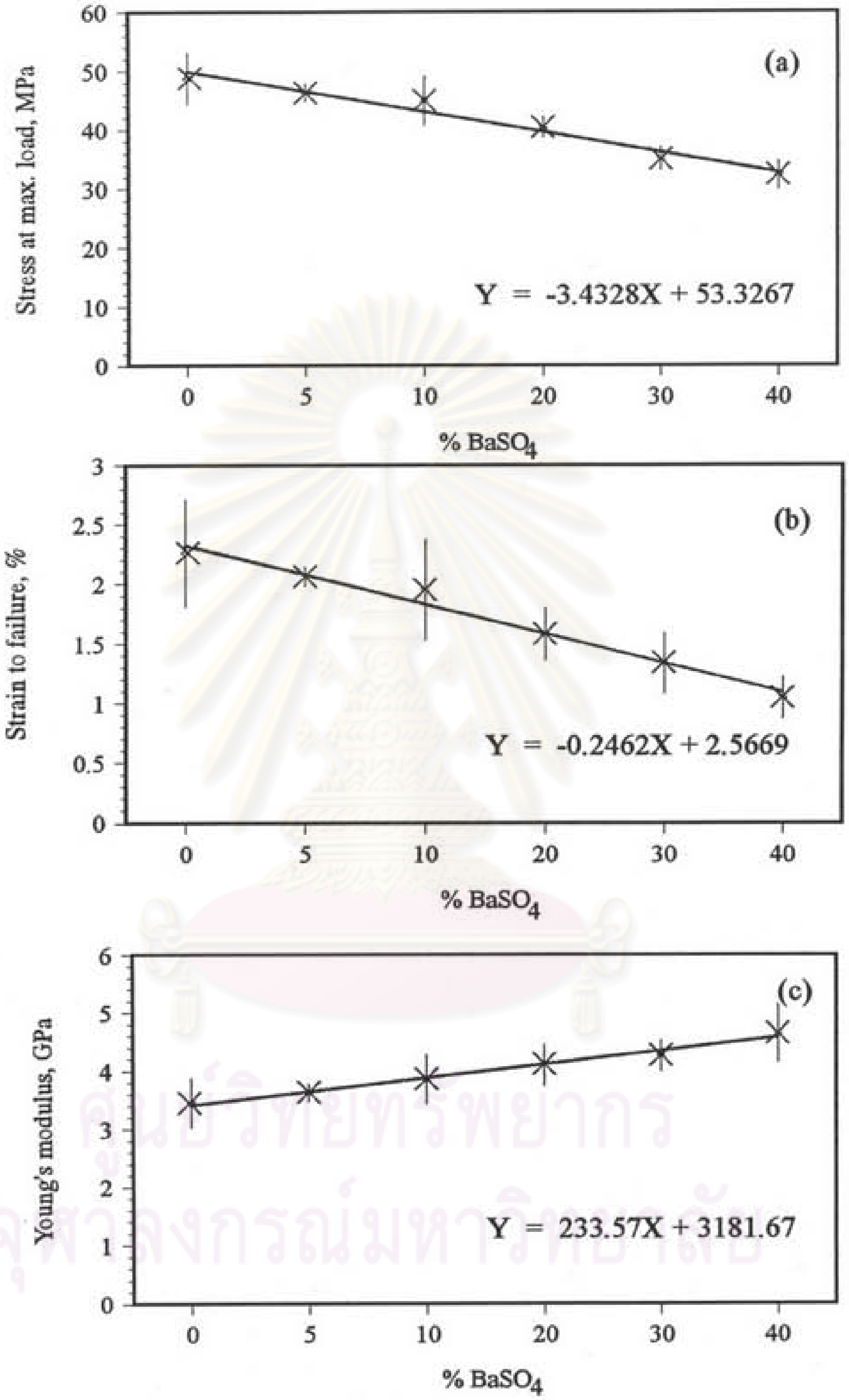

Figure 4.9 Tensile properties of PMMA-Co-PEMA dependence with increasing percent weight of $BaSO_4$(a) Stress at maximum load (b) Strain to faliure (c) Young's modulus

4.6 Mechanical Properties of Hydroxyapatite Reinforced PMMA-Co-PEMA Bone Cement

It has been reported that hydroxyapatite not only improves mechanical properties of bone cements but also introduces interfacial bone between the bone cement and bone tissue(82-89). Therefore, mechanical properties of hydroxyapatite reinforced copolymer bone cement was also investigated and shown in Table 4.5 and Figure 4.10. The Young's modulus was observed to increase upto 39 % from 3453 MPa to 4802 MPa for 0-40 weight percent ranges of hydroxyapatite.

Table 4.5 Tensile properties of untreated hydroxyapatite reinforced PMMA-Co-PEMA

HAP %	Stress, MPa (at max. load)		Strain to failure, %		Modulus, MPa	
0	48.77	(8.89)	2.26	(19.93)	3453	(12.09)
5	46.88	(10.05)	1.92	(34.19)	3861	(9.50)
10	45.32	(8.76)	1.88	(22.13)	4084	(14.04)
20	41.12	(8.45)	1.60	(20.64)	4408	(12.41)
30	38.17	(10.48)	1.31	(18.86)	4746	(7.24)
40	34.49	(8.88)	0.94	(28.01)	4802	(7.65)

NOTE : ( ) is coefficient of variation

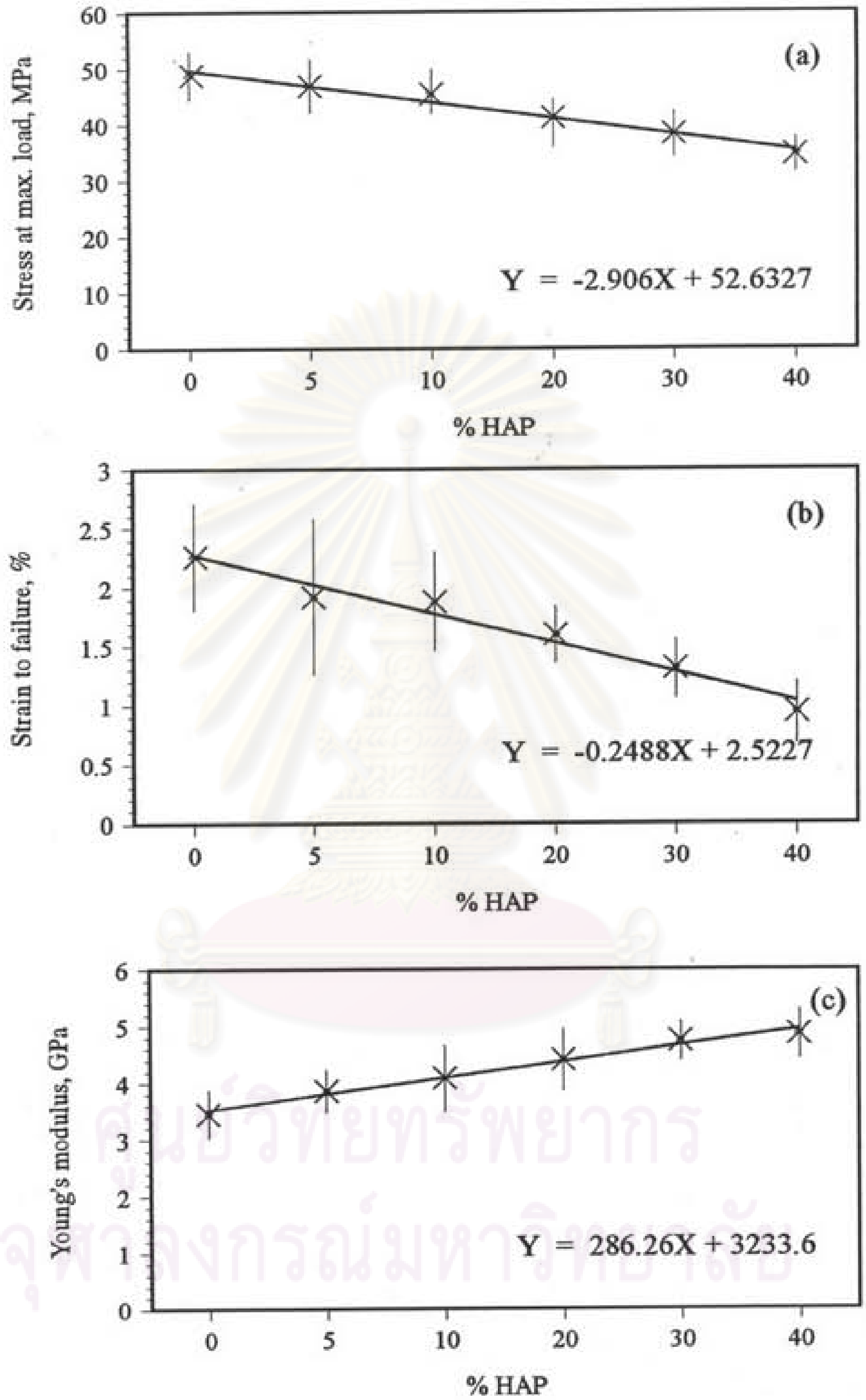

Figure 4.10 Tensile properties of PMMA-Co-PEMA dependence with increasing percent weight of untreated HAP (a) Stress at maximum load (b) Strain to failure (c) Young's modulus

4.7 Mechanical Properties of Silane-Treated Hydroxyapatite Reinforced PMMA-Co-PEMA Bone Cement

With the introduction of silane treated hydroxyapatite to the PMMA-Co-PEMA bone cement, an enhancement of tensile properties was observed as a direct consequence of the chemical bonding between the hydroxyapatite and PMMA-Co-PEMA. Dependence of Young's modulus of the bone cement upon hydroxyapatite content from 0 to 40 % by weight with various contents of silane coupling agent was illustrated in Figure 4.11-4.13. The Young's modulus was observed to be increased from 3453 to 5221 MPa, from 3453 to 5535 MPa, and from 3453 to 5240 MPa for 3.72, 5.21, and 7.83 % silane content, as shown in Table 4.6-4.8, respectively. It was observed that Young's modulus of the copolymer increased with increasing weight percent of hydroxyapatite reinforcement and tended to be maximum when the hydroxyapatite had silane content about 5 % by weight, as shown in Figure 4.14.

Table 4.6 Tensile properties of PMMA-Co-PEMA bone cement reinforced with hydroxyapatite having 3.72 weight percent silane content

HAP %	Stress, MPa (at max. load)		Strain to failure, %		Modulus, MPa	
0	48.77	(8.89)	2.26	(19.93)	3453	(12.09)
5	46.98	(7.56)	1.96	(21.32)	3913	(5.71)
10	40.48	(11.39)	1.63	(23.14)	4116	(10.39)
20	38.10	(10.62)	1.31	(24.45)	4415	(10.40)
30	33.80	(9.49)	1.05	(30.28)	5051	(7.40)
40	30.91	(10.48)	0.90	(12.42)	5221	(12.96)

NOTE : ( ) is coefficient of variation

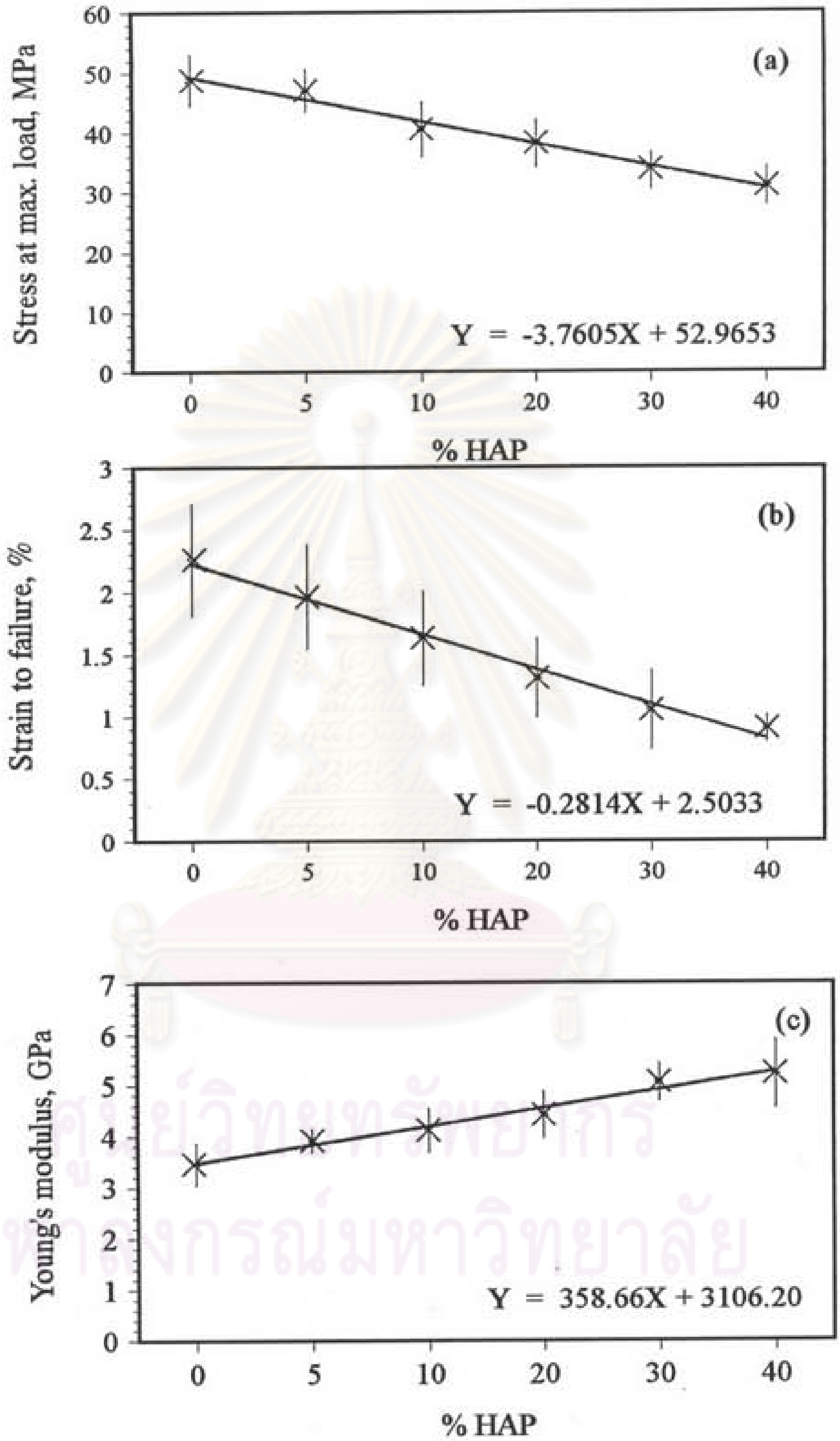

Figure 4.11 Tensile properties of PMMA-Co-PEMA dependence with increasing weight percent of hydroxyapatite having 3.72 weight percent silane content (a) Stress at maximum load (b) Strain to failure (c) Young's modulus

Table 4.7 Tensile properties of PMMA-Co-PEMA bone cement reinforced with hydroxyapatite having 5.21 weight percent silane content

HAP %	Stress, MPa (at max. load)		Strain to failure, %		Modulus, MPa	
0	48.77	(8.89)	2.26	(19.93)	3453	(12.09)
5	48.47	(7.67)	2.19	(25.59)	4424	(8.30)
10	44.37	(6.70)	1.65	(16.24)	4506	(8.82)
20	42.82	(8.98)	1.56	(21.36)	4731	(12.60)
30	37.23	(6.80)	1.10	(30.96)	5305	(13.23)
40	32.28	(11.79)	0.87	(17.79)	5535	(12.55)

NOTE : ( ) is coefficient of variation

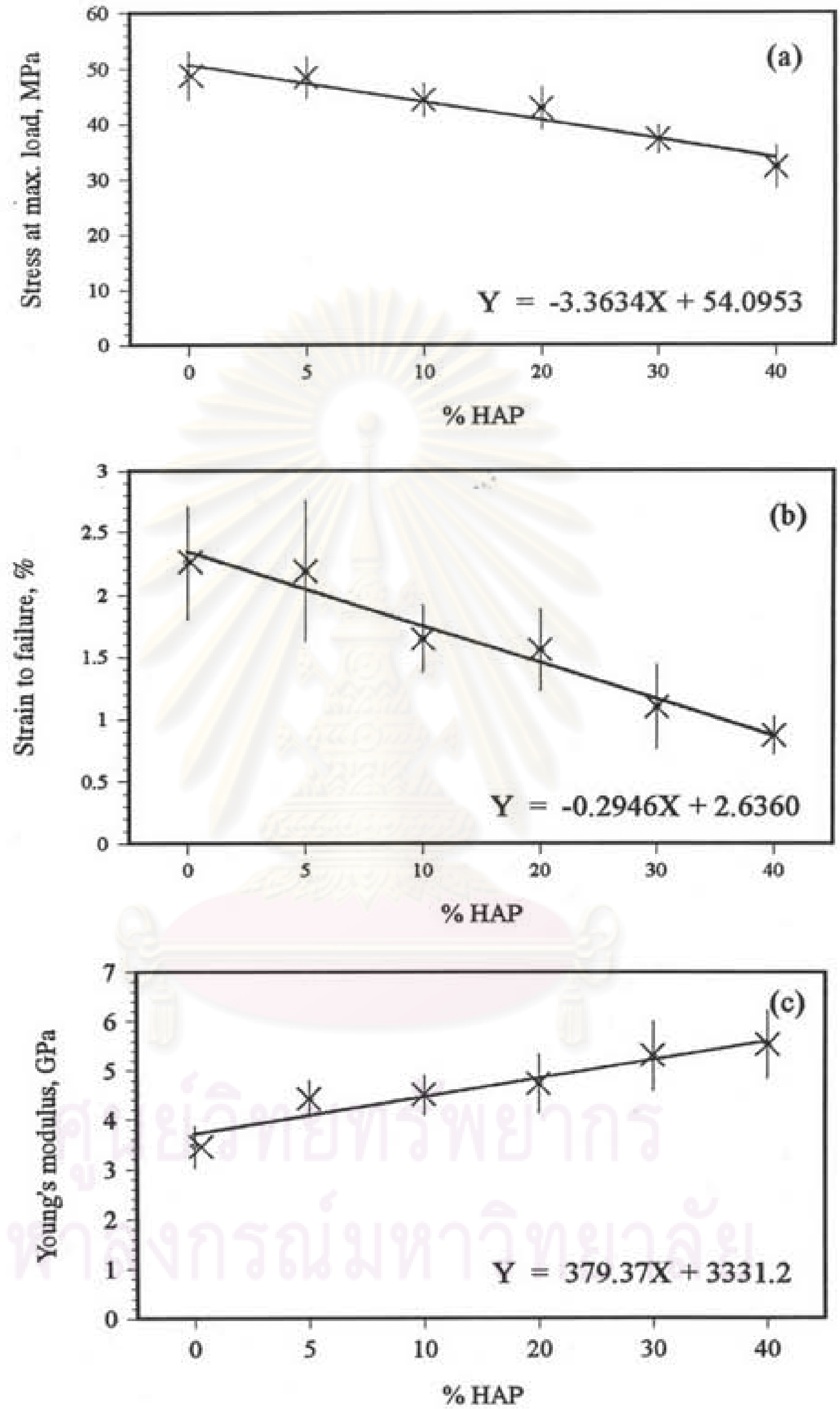

Figure 4.12 Tensile properties of PMMA-Co-PEMA dependence with increasing weight percent of hydroxyapatite having 5.21 weight percent silane content (a) Stress at maximum load (b) Strain to failure (c) Young's modulus

Table 4.8 Tensile properties of PMMA-Co-PEMA bone cement reinforced with hydroxyapatite having 7.83 weight percent silane content

HAP %	Stress, MPa (at max. load)		Strain to failure, %		Modulus, MPa	
0	48.77	(8.89)	2.26	(19.93)	3453	(12.09)
5	46.92	(8.11)	2.27	(18.85)	4080	(10.05)
10	43.09	(9.12)	1.82	(17.41)	4214	(4.59)
20	38.03	(14.89)	1.30	(36.13)	4537	(11.95)
30	34.72	(9.10)	1.00	(33.54)	5203	(8.58)
40	33.60	(14.14)	0.91	(24.90)	5240	(10.51)

NOTE : ( ) is coefficient of variation

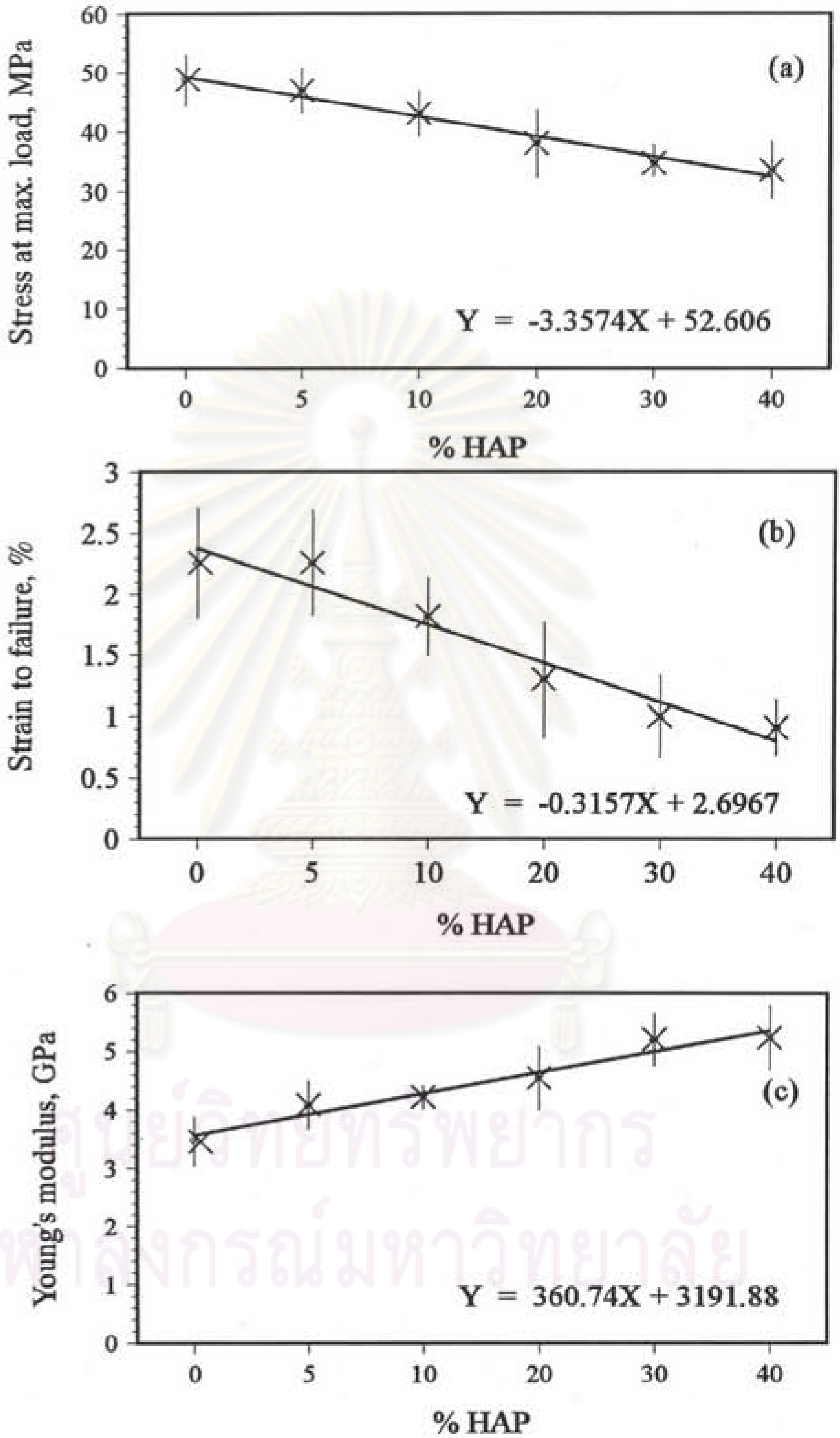

Figure 4.13 Tensile properties of PMMA-Co-PEMA dependence with increasing weight percent of hydroxyapatite having 7.83 weight percent content (a) Stress at maximum load (b) Strain to failure (c) Young's modulus

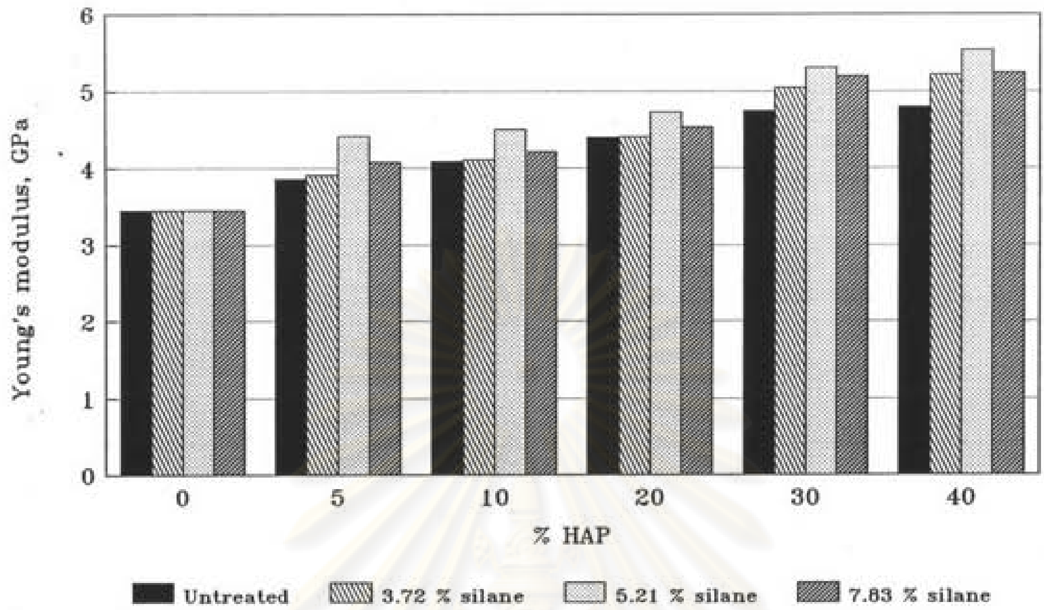

Figure 4.14 Comparison between Young's modulus of the PMMA-Co-PEMA with increasing weight percent of hydroxyapatite reinforcement

Comparison of tensile properties between the untreated hydroxyapatite modified bone cement and 5.21 weight percent of silane treated hydroxyapatite, was observed that Young's modulus increased by approximately 13 % for similar weight percent changes in hydroxyapatite.

Note: The result of specimens tested with Instron universal testing machine, showed in appendix A, was similar to those obtained from Lloyd universal testing machine.

4.8 Void Content in the Bone Cement Specimens

It was observed from Table 4.9 that void content was rather low in case of pure bone cements, but higher in case of the bone cements reinforced with either BaSO4 or hydroxyapatite. It was also observed that the bone cements reinforced with silane-treated hydroxyapatite had lower void content than those reinforced with untreated hydroxyapatite. These results indicate dependence of void content on compatibility between the bone cement matrix and the reinforcement. Moreover, it was observed that void content distributed so much which may be considered as a result of hand mixing.

Due to large distribution of void content, dependence of void content on amount of reinforcement cannot be determined. As higher void content will result to lower mechanical strength, void content in each specimen should be determined consequently with the mechanical properties.

Table 4.9 Void content of bone cement specimens

Pure PMMA	weight (g)				Void content
	in air	in water	before ignition	after ignition	% by volume
1	0.1609	0.0273			0.54
2	0.0937	0.0164			0.37
3	0.1313	0.0220			0.42
4	0.0764	0.0135			0.31
5	0.1328	0.0248			0.68
6	0.1324	0.0229			0.49
7	0.1249	0.0224			0.54
8	0.1444	0.0260			0.64
PMMA + $BaSO_4$ 10 %					
1	0.1728	0.0322	21.3000	21.1377	2.64
2	0.1313	0.0244	21.0336	20.9103	2.71
3	0.1121	0.0232	20.7901	20.6839	-0.45
4	0.1487	0.0304	19.8793	19.7404	0.78
5	0.1269	0.0264	20.1483	20.0310	0.99
6	0.1406	0.0265	22.3738	22.2432	3.08
7	0.1323	0.0259	20.9270	20.8031	1.68
8	0.1185	0.0235	20.3714	20.2614	1.93
PMMA + $BaSO_4$ 20 %					
1	0.1329	0.0310	20.5715	20.4566	1.97
2	0.1449	0.0355	20.7318	20.6074	0.88
3	0.1423	0.0330	20.6565	20.5344	2.61
4	0.1629	0.0381	20.2541	20.1123	1.47
5	0.1451	0.0337	22.2929	22.1678	2.27
6	0.1676	0.0367	22.2878	22.1418	3.31
7	0.1331	0.0309	20.3632	20.2468	1.41
8	0.1269	0.0283	23.0289	22.9183	2.78
PMMA + $BaSO_4$ 30 %					
1	0.1464	0.0412	20.9239	20.8058	-0.22
2	0.1314	0.0361	21.0456	20.9405	1.21
3	0.1474	0.0404	21.8939	21.7359	-19.05
4	0.1751	0.0464	20.1165	19.9752	2.00
5	0.1833	0.0513	32.8191	32.6823	4.55
6	0.1967	0.0547	22.5028	22.3471	1.38
PMMA + $BaSO_4$ 40 %					
1	0.1686	0.0549	32.9043	32.7823	-0.10
2	0.1666	0.0533	24.3390	24.2169	0.00
3	0.1600	0.0520	32.9244	32.8072	-0.72
4	0.1623	0.0523	31.9060	31.7873	-0.22
5	0.1288	0.0421	26.8120	26.7186	-0.41
6	0.1661	0.0547	34.1669	34.0519	1.88
7	0.1577	0.0483	26.6060	26.4889	1.21

Table 4.9 Void content of bone cement specimens (continued)

Pure PMMA-Co-PEMA	weight (g)				Void content
	in air	in water	before ignition	after ignition	% by volume
1	0.1152	0.0187			0.31
2	0.1525	0.0261			0.54
3	0.1064	0.0180			0.35
4	0.1456	0.0237			0.39
5	0.1413	0.0239			0.47
6	0.1224	0.0201			0.35
7	0.1449	0.0251			0.54
8	0.1619	0.0277			0.57
PMMA-Co-PEMA + $BaSO_4$ 5 %					
1	0.1371	0.0263	25.9427	25.8100	-0.78
2	0.1227	0.0225	26.1798	26.0622	0.91
3	0.1708	0.0303	25.8785	25.7130	0.92
4	0.1282	0.0239	25.6746	25.5497	-0.54
5	0.1321	0.0248	28.8825	28.7559	0.38
6	0.1504	0.0285	31.9690	31.8245	0.00
PMMA-Co-PEMA + $BaSO_4$ 10 %					
1	0.1328	0.0244	27.7063	27.5815	2.12
2	0.1476	0.0287	25.8039	25.6652	0.82
3	0.1110	0.0224	33.5794	33.4747	-0.34
4	0.1710	0.0340	32.3874	32.2287	1.08
5	0.1198	0.0239	31.7223	31.6101	0.41
6	0.1204	0.0239	24.1692	24.0534	-1.20
7	0.1246	0.0226	25.8366	25.7184	1.81
8	0.1227	0.0222	32.5964	32.4806	2.19
PMMA-Co-PEMA + $BaSO_4$ 20 %					
1	0.1366	0.0324	28.8889	28.7705	0.53
2	0.1347	0.0321	34.1447	34.0282	0.52
3	0.1368	0.0314	25.6826	25.5646	1.81
4	0.1361	0.0327	22.2839	22.1658	0.05
5	0.1435	0.0346	20.2327	20.1096	0.66
6	0.1856	0.0451	23.0858	22.9267	0.46
PMMA-Co-PEMA + $BaSO_4$ 30 %					
1	0.1513	0.0416	20.5895	20.4703	1.33
2	0.1427	0.0390	21.8488	21.7344	0.51
3	0.1750	0.0488	20.9702	20.8316	0.48
4	0.1774	0.0502	22.2957	22.1559	0.21
5	0.1471	0.0427	20.9227	20.8062	-1.12
PPMA-Co-PEMA + $BaSO_4$ 40 %					
1	0.1496	0.0495	22.3850	22.2772	-1.39
2	0.1782	0.0570	21.8842	21.7566	0.62
3	0.1509	0.0478	23.0529	22.9446	0.94
4	0.1513	0.0492	20.3818	20.2720	-0.95
5	0.1465	0.0478	20.4006	20.2958	-0.27
6	0.1655	0.0471	22.3145	22.1955	5.29
7	0.1466	0.0461	20.2378	20.1321	1.01
8	0.1735	0.0545	22.4808	22.3570	1.66

Table 4.9 Void content of bone cement specimens (continued)

PMMA-Co-PEMA + HAP 5 %	weight (g)				Void Content % by volume
	in air	in water	before ignition	after ignition	
1	0.1110	0.0178	21.0144	20.9061	2.34
2	0.1227	0.0193	25.6697	25.5497	2.56
3	0.1441	0.0235	31.9665	31.8254	1.81
4	0.1068	0.0161	34.1172	34.0135	3.72
5	0.1585	0.0258	25.8156	25.6613	2.19
6	0.0905	0.0134	28.8435	28.7551	3.68
7	0.1259	0.0210	26.5710	26.4486	1.79
8	0.1004	0.0146	33.5711	33.4716	3.15
PMMA-Co-PEMA + HAP 10 %					
1	0.1484	0.0275	24.3204	24.1811	1.61
2	0.1332	0.0243	32.7775	32.6513	1.42
3	0.1068	0.0212	25.8170	25.7162	-0.33
4	0.1220	0.0229	22.2417	22.1254	0.42
5	0.1379	0.0247	21.8437	21.7120	1.36
6	0.1097	0.0207	20.9051	20.8003	0.18
7	0.1226	0.0226	20.5629	20.4452	0.42
8	0.1205	0.0218	22.4290	22.3133	0.83
PMMA-Co-PEMA + HAP 20 %					
1	0.1652	0.0358	25.9724	25.8302	2.61
2	0.1353	0.0293	32.8998	32.7822	2.10
3	0.1245	0.0267	25.8544	25.7264	-7.71
4	0.1323	0.0268	32.6070	32.4927	4.14
5	0.1033	0.0217	32.7472	32.6567	2.46
6	0.1342	0.0281	32.8723	32.7556	2.96
7	0.1453	0.0308	20.9214	20.7952	2.70
8	0.1339	0.0285	24.3062	24.1894	2.36
PMMA-Co-PEMA + HAP 30 %					
1	0.1939	0.0434	26.2547	26.0995	5.58
2	0.1279	0.0259	22.4351	22.3322	7.85
3	0.1215	0.0303	20.5609	20.4630	2.02
4	0.1478	0.0369	26.8336	26.7152	2.29
5	0.1376	0.0350	32.3543	32.2436	1.45
6	0.1221	0.0303	20.1448	20.0478	2.92
7	0.1156	0.0275	19.8479	19.7554	3.86
8	0.1075	0.0266	21.2338	21.1474	2.40
PMMA-Co-PEMA + HAP 40 %					
1	0.1311	0.0346	25.6781	25.5810	4.48
2	0.1285	0.0353	21.0421	20.9480	3.63
3	0.1537	0.0422	21.0572	20.9440	3.36
4	0.1268	0.0363	19.8604	19.7661	1.28
5	0.1180	0.0314	21.2442	21.1579	4.83
6	0.1339	0.0370	20.9098	20.8108	2.93
7	0.1674	0.0440	28.9206	28.7962	4.45
8	0.1577	0.0420	25.8150	25.6988	4.42

Table 4.9 Void content of bone cement specimens (continued)

PMMA-Co-PEMA + HAP 5%-silane 3.72%	weight (g)				Void content % by volume
	in air	in water	before ignition	after ignition	
1	0.1454	0.0261	27.7197	27.5774	-0.12
2	0.1069	0.0185	32.3256	32.2200	0.11
3	0.1161	0.0195	31.7200	31.6060	1.07
4	0.1260	0.0205	21.0394	20.9158	1.75
5	0.1161	0.0190	20.9105	20.7969	1.79
6	0.1241	0.0214	20.7123	20.5908	0.71
7	0.1070	0.0151	22.2261	22.1212	4.26
8	0.1119	0.0169	20.0520	19.9416	2.77
PMMA-Co-PEMA + HAP 10%-silane 3.72%					
1	0.1007	0.0183	21.2270	21.1309	1.09
2	0.1174	0.0199	27.6780	27.5789	9.14
3	0.1170	0.0210	33.5868	33.4742	0.87
4	0.1180	0.0231	25.7749	25.6620	-0.79
5	0.1240	0.0205	32.3425	32.2240	2.95
6	0.1020	0.0166	31.7058	31.6079	3.00
7	0.1037	0.0183	26.5492	26.4495	1.29
8	0.1304	0.0234	31.9521	31.8274	1.24
PMMA-Co-PEMA + HAP 20%-silane 3.72%					
1	0.0857	0.0180	31.6908	31.6116	-0.56
2	0.1224	0.0255	31.9450	31.8326	0.03
3	0.1366	0.0293	34.1480	34.0229	-0.60
4	0.1066	0.0226	26.5522	26.4558	0.44
5	0.1047	0.0213	32.3231	32.2275	0.97
6	0.1143	0.0228	27.6885	27.5847	1.76
7	0.1225	0.0241	33.5919	33.4798	1.67
8	0.1026	0.0200	22.4087	22.3173	3.39
PMMA-Co-PEMA + HAP 30%-silane 3.72%					
1	0.1175	0.0252	32.5912	32.4944	5.23
2	0.1348	0.0313	26.1988	26.0832	0.85
3	0.0980	0.0222	32.7406	32.6601	3.90
4	0.1135	0.0262	26.7979	26.7040	2.98
5	0.1304	0.0278	21.2564	21.1481	4.96
6	0.1213	0.0260	21.0239	20.9233	4.89
7	0.1091	0.0244	20.7862	20.6956	3.68
8	0.1117	0.0246	19.8436	19.7513	4.37
PMMA-Co-PEMA + HAP 40%-silane 3.72%					
1	0.1079	0.0277	33.5771	33.4937	3.24
2	0.1124	0.0295	25.7696	25.6827	2.48
3	0.1455	0.0380	31.7499	31.6365	2.23
4	0.1112	0.0274	26.5568	26.4702	4.18
5	0.1011	0.0222	28.8541	28.7755	7.56
6	0.1332	0.0356	21.0360	20.9337	2.19
7	0.1208	0.0337	20.8970	20.8042	0.58
8	0.1091	0.0285	20.1330	20.0486	2.61

Table 4.9 Void content of bone cement specimens (continued)

PMMA-Co-PEMA + HAP 5%-silane 5.21%	weight (g)				Void content % by volume
	in air	in water	before ignition	after ignition	
1	0.1003	0.0197	34.1093	34.0126	-1.33
2	0.1521	0.0272	32.9155	32.7691	0.94
3	0.1126	0.0207	24.2835	24.1750	0.27
4	0.1001	0.0188	25.9059	25.8096	-0.13
5	0.0978	0.0163	25.8065	25.7119	2.10
6	0.0997	0.0171	32.8362	32.7400	1.67
7	0.0944	0.0159	31.8375	31.7466	2.15
8	0.0958	0.0174	22.4017	22.3092	0.42
PMMA-Co-PEMA + HAP 10%-silane 5.21%					
1	0.0957	0.0178	22.2433	22.1538	1.74
2	0.1052	0.0180	22.2243	22.1258	3.44
3	0.1047	0.0200	20.3335	20.2353	0.96
4	0.0875	0.0163	22.9886	22.9066	1.58
5	0.1209	0.0222	21.0344	20.9213	2.01
6	0.0987	0.0180	21.8037	21.7110	1.93
7	0.0994	0.0184	20.0392	19.9461	1.76
8	0.1253	0.0228	31.8695	31.7520	2.07
PMMA-Co-PEMA + HAP 20%-silane 5.21%					
1	0.1024	0.0229	23.0040	22.9141	0.64
2	0.1232	0.0293	20.7124	20.6041	-1.28
3	0.0963	0.0230	20.3251	20.2410	-1.04
4	0.1267	0.0294	20.2172	20.1068	-0.02
5	0.1830	0.0408	20.4375	20.2783	1.24
6	0.1177	0.0262	22.2656	22.1629	1.12
7	0.1284	0.0298	20.0683	19.9563	-0.09
8	0.1063	0.0243	22.3405	22.2474	0.14
PMMA-Co-PEMA + HAP 30%-silane 5.21%					
1	0.1052	0.0266	21.8104	21.7258	1.67
2	0.1226	0.0325	22.2423	22.1442	0.30
3	0.1202	0.0314	22.3547	22.2582	0.64
4	0.1174	0.0315	20.0575	19.9630	-0.46
5	0.1193	0.0302	20.3488	20.2526	1.48
6	0.0996	0.0271	22.4069	22.3269	-0.87
7	0.1360	0.0370	20.9306	20.8220	-0.54
8	0.1332	0.0358	20.7216	20.6158	0.20
PMMA-Co-PEMA + HAP 40%-silane 5.21%					
1	0.1186	0.0347	20.3723	20.2865	1.82
2	0.1063	0.0308	21.0197	20.9419	1.62
3	0.1223	0.0352	21.2487	21.1600	2.35
4	0.1367	0.0387	19.8703	19.7694	2.10
5	0.0914	0.0267	31.9132	31.8453	0.52
6	0.1171	0.0338	32.3364	32.2493	0.94
7	0.1095	0.0323	34.1208	34.0396	0.21
8	0.0901	0.0275	27.6649	27.5986	-0.85

Table 4.9 Void content of bone cement specimens (continued)

PMMA-Co-PEMA + HAP 5%-silane 7.83%	weight (g)				Void content
	in air	in water	before ignition	after ignition	% by volume
1	0.1160	0.0199	25.8260	25.7122	0.70
2	0.1278	0.0226	32.8924	32.7672	0.14
3	0.1088	0.0177	32.5838	32.4773	1.88
4	0.1023	0.0185	24.2765	24.1745	-1.40
5	0.0924	0.0164	26.7782	26.6874	-0.12
6	0.0979	0.0176	19.8304	19.7345	-0.21
7	0.1098	0.0192	21.0128	20.9058	0.69
8	0.1013	0.0186	20.1249	20.0262	-0.36
PMMA-Co-PEMA + HAP 10%-silane 7.83%					
1	0.0996	0.0180	31.8441	31.7495	1.48
2	0.1068	0.0204	25.9141	25.8134	0.66
3	0.1156	0.0202	32.8536	32.7438	2.20
4	0.1034	0.0192	26.1641	26.0661	1.01
5	0.1062	0.0203	26.7919	26.6913	0.37
6	0.1115	0.0212	32.3283	32.2225	0.39
7	0.1140	0.0221	32.8794	32.7709	-0.24
8	0.0912	0.0172	32.5671	32.4799	0.14
PMMA-Co-PEMA + HAP 20%-silane 7.83%					
1	0.1795	0.0404	32.3969	32.2410	1.06
2	0.1208	0.0267	31.7235	31.6183	1.43
3	0.1214	0.0270	22.3555	22.2499	1.32
4	0.1400	0.0308	20.8945	20.8128	19.87
5	0.1329	0.0313	20.3929	20.2719	-3.02
6	0.1191	0.0266	20.7075	20.6040	1.25
7	0.1359	0.0293	20.6512	20.5316	1.53
8	0.1330	0.0284	20.2232	20.1074	2.38
PMMA-Co-PEMA + HAP 30%-silane 7.83%					
1	0.1369	0.0353	25.9442	25.8339	0.90
2	0.1503	0.0386	31.8944	31.7730	0.90
3	0.1170	0.0300	32.8547	32.7598	0.73
4	0.1023	0.0245	20.5405	20.4588	3.76
5	0.1253	0.0306	20.9007	20.8003	2.98
6	0.1250	0.0314	32.3419	32.2411	1.74
7	0.1211	0.0285	32.7650	32.6669	3.53
8	0.1038	0.0247	26.1645	26.0805	3.26
PMMA-Co-PEMA + HAP 40%-silane 7.83%					
1	0.1068	0.0302	20.1302	20.0515	2.23
2	0.0901	0.0253	26.5346	26.4680	2.34
3	0.1373	0.0381	25.6833	25.5826	3.18
4	0.1379	0.0385	28.8900	28.7886	2.82
5	0.1072	0.0300	31.9278	31.8485	2.43
6	0.1087	0.0308	27.6825	27.6022	2.02
7	0.1351	0.0392	25.7911	25.6919	1.40
8	0.1084	0.0299	33.5768	33.4964	2.84